Chapter 2
Theory and Model

2.1 Theory

The barotropic free oscillations of the global ocean are defined through the linearized homogeneous shallow water equations (e.g. [57]).

$$\frac{\partial \mathbf{v}}{\partial t} + \mathbf{f} \times \mathbf{v} + \frac{r'}{D}\mathbf{v} + \mathbf{F} + g\nabla\zeta + \mathbf{L}_{sek} = 0$$
$$\frac{\partial \zeta}{\partial t} + \nabla \cdot (D\mathbf{v}) = 0, \tag{2.1}$$

where ζ denotes the sea surface elevation with respect to the moving sea bottom, $\mathbf{v} = (u, v)$ the horizontal current velocity vector. The undisturbed ocean depth is D, the vector of Coriolis acceleration $\mathbf{f} = 2\omega \sin\phi \mathbf{z}$, the coefficient of linear bottom friction r' and the gravitational acceleration g. $\mathbf{F}$ denotes the vector defining the second-order eddy viscosity term $(F_\lambda, F_\phi) = (-A_h \Delta u, -A_h \Delta v)$ and (λ, ϕ) a set of geographic longitude and latitude values. $\mathbf{L}_{sek}$ is the vector of the secondary force of the loading and self-attraction (LSA), it is derived in section 2.1.1.
In spherical coordinates this system of equations is written as:

$$\frac{\partial u}{\partial t} - 2\omega \sin\phi \cdot v + \frac{r'}{D} \cdot u - A_h \Delta_H u + \frac{g}{R\cos\phi}\frac{\partial \zeta}{\partial \lambda} + L_{sek,\lambda} = 0 \tag{2.2}$$

$$\frac{\partial v}{\partial t} + 2\omega \sin\phi \cdot u + \frac{r'}{D} \cdot v - A_h \Delta_H v + \frac{g}{R}\frac{\partial \zeta}{\partial \phi} + L_{sek,\phi} = 0 \tag{2.3}$$

$$\frac{\partial \zeta}{\partial t} + \frac{1}{R\cos\phi}\left(\frac{\partial (Du)}{\partial \lambda} + \frac{\partial (Dv\cos\phi)}{\partial \phi}\right) = 0 \tag{2.4}$$

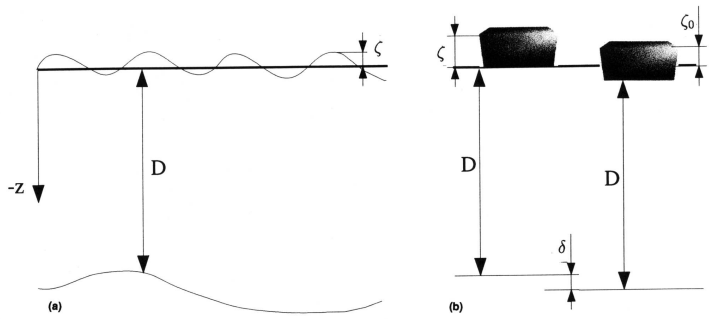

Fig. 2.1 (a) A sketch explaining the used variables z, D, and ζ : the negative z-axis is in downward direction starting from the undisturbed sea-level (z=0), the sea surface deformation ζ is in upward direction also starting from (z=0). The ocean depth D is the distance between the undisturbed sea-level down to the ocean bottom. (b) **left**: Sea surface deformation ζ without a deformation of the ocean bottom. **right**: The deformation δ of the sea bottom through mass loading. ζ_0 is the geocentric sea level . The distance from the undisturbed sea level to the ocean bottom is now $D-\delta$.

2.1.1 Secondary Forces: The Loading and Self-Attraction Effect

External forces are e.g. tidal forces, atmospheric pressure and wind stress. They have in common that they do not interact in the first order with the ocean dynamics and thus are controlled independently. Against that, the secondary forces have their origin in the dynamics of the water masses and interact with them. In this study the focus is on the secondary forces of loading and self-attraction. The loading-effect results from the deformation of the elastic earth due to the variations of the vertical extension of the water column. The self-attraction is due to the gravitational interaction of the watermasses with themselves. All in all this effect is called the loading and self-attraction effect. This secondary force is derived in terms of the variation of a potential:
Both components of the LSA-effect depend on the sea surface elevation ζ related to the undisturbed sea level and to the actual ocean bottom, i.e. being defined as the variation of the height of the water column (Fig. 2.1a). ζ is written in spherical harmonics:

$$\zeta = \sum_{n=0}^{\infty} \zeta_n = \sum_{n=0}^{\infty} \sum_{s=0}^{n} \overline{P}_{n,s} \left[C_{n,s} \cos s\lambda + S_{n,s} \sin s\lambda \right] \tag{2.5}$$

There,

$$\overline{P}_{n,s} = \left(\frac{2(2n+1)}{\delta_s} \frac{(n-s)!}{(n+s)!} \right)^{\frac{1}{2}} P_{n,s}; \qquad \delta_s = 2(s=0), \delta_s = 1(s>0)$$

are the associated Legendre Functions. $C_{n,s}$ and $S_{n,s}$ are time dependent coefficients.

Self-Attraction Effect

Firstly, the elasticity of the earth is neglected, in order to derive solely the expression of the potential of the self-attraction effect. The potential of a spherical layer is given through (Fig. 2.2):

$$\Phi(M) = \gamma \int \int_{\delta K_R} \frac{\rho(M')}{\overline{MM'}} dS$$

There, δK_R is a spherical layer and $\rho(M')$ is the area density. The distance of the masses M and M' to the center of the sphere is r and R, respectively. Transformation of the reciprocal distance $\overline{MM'}^{-1}$ in spherical harmonics [45] yields:

$$\frac{1}{\overline{MM'}} = (R^2 - 2Rr\cos\alpha + r^2)^{-\frac{1}{2}} = \sum_{n=0}^{\infty} P_n(\cos\alpha)\frac{r^n}{R^{n+1}}, with \quad r < R$$

Using the notation $f(\lambda', \phi') := \rho(M')$ and considering the area elements $dS = R^2 \sin\phi' d\phi' d\lambda'$ yields

$$\Phi(M) = \gamma \sum_{n=0}^{\infty} \frac{r^n}{R^{n+1}} \int \int_{\delta K_R} f(\lambda', \phi') P_n(\cos\alpha) dS.$$

The area density is now written in spherical harmonics $f(\lambda, \phi) = \sum_{n=0}^{\infty} f_n(\lambda, \phi)$ with $f_n(\lambda, \phi) = \frac{2n+1}{4\pi} \int \int_{\delta K_R} f(\lambda', \phi') P_n(\cos\alpha) dS$. Thus, the potential is rewritten in

$$\Phi(M) = 4\pi\gamma \sum_{n=0}^{\infty} \frac{r^n}{R^{n-1}} f_n(\lambda, \phi).$$

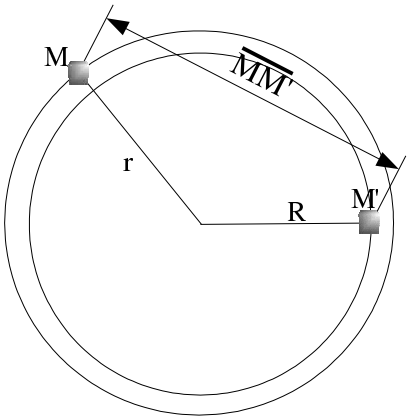

Fig. 2.2 The potential of a spherical layer: The mass M in the potential of the surrounding masses M' ($\Phi(M) = \gamma \int \int_{\delta K_R} \frac{\rho(M')}{\overline{MM'}} dS$).

Since the radius of the earth R is large compared to the ocean depth, for the radius r holds $r \to R$ and the area density can be approximated through $f(\lambda,\phi) = \rho\zeta(\lambda,\phi)$ with constant distance to the earth's center R. Finally, the potential can be written as

$$\Phi(\phi,\lambda) = g \cdot \sum_{n=0}^{\infty} \frac{3}{2n+1} \frac{\rho_0}{\rho_e} \zeta_n(\phi,\lambda) =: \sum_{n=0}^{\infty} \Phi_n(\phi,\lambda) \tag{2.6}$$

ρ_0 and ρ_e are the mean densities of the sea water and the solid earth, respectively. This potential describes the so called self-attraction effect. The gradient of this potential is the gravitative force of the watermasses on themselves.

Loading-Effect

Hereafter it is assumed that the earth is fully elastic. Thus, the ocean bottom gets deformed through forces acting on it. In the present study only inner forces can deformate the ocean bottom, external forces are excluded in the homogeneous problem of determining free oscillations. The surface elevation ζ gives rise to two forces; on the one hand the changing weight of the water column, on the other hand the changing gravitational attraction on the ocean bottom.
The spherical harmonic of degree n of the geocentric sea surface elevation is $(\zeta_0)_n$ (compare 2.5), and the deformation of the ocean bottom is described through δ (Fig. 2.1b).
Compared to the undisturbed sea level ($\zeta = 0$), the additional body of water

$$g\rho\zeta_n = g\rho(\zeta_0 - \delta)_n$$

deformates the ocean bottom due to the two abovementioned inner forces. [9] showed that the vertical displacement of the ocean bottom δ_n is proportional to the vertical expansion of the water column. The factor of proportionality is h'_n:

$$\delta_n = h'_n \cdot \frac{3}{2n+1} \frac{\rho_0}{\rho_e} \zeta_n = h'_n \Phi_n / g \tag{2.7}$$

Since the pressure through the loading overbalances the gravitational attraction, the h'_n are negative for all degrees n. The mass displacement through the deformation of the ocean bottom results additionally in a variation of the potential. This can be described by the factor of proportionality k'_n:

$$V'_n = k'_n \cdot \Phi_n \tag{2.8}$$

These parameters, h'_n and k'_n, depend on the characteristics of the elasticity of the earth and are called the loading Love-numbers . They describe the interaction of the ocean with the solid earth in terms of spherical harmonics.
The loading Love-numbers used in this study are taken from [10]. They determined the Love-numbers values taking the Preliminary Reference Earth Model (PREM) [5]

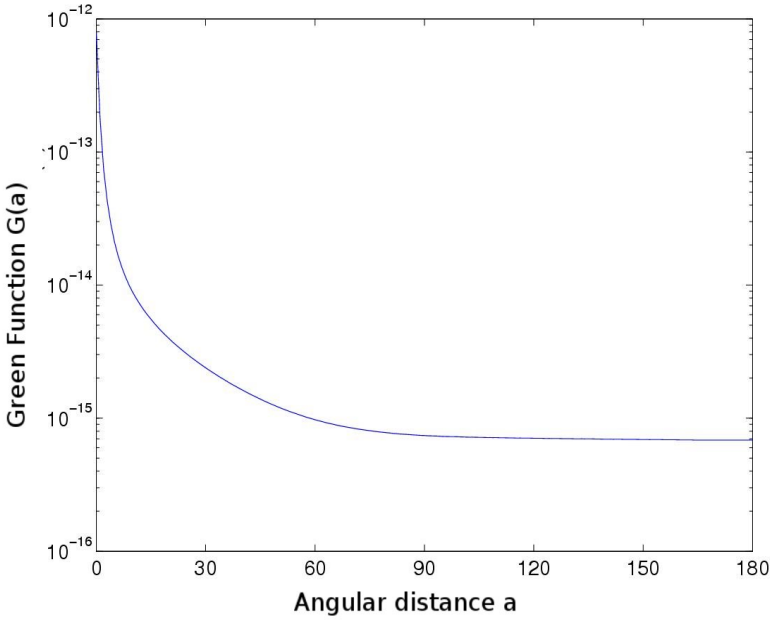

Fig. 2.3 The Green's function depending on the angular distance a between the two points (ϕ, λ) and (ϕ', λ'). It holds for the angular distance: $(\cos(a) = \sin\phi \sin\phi' + \cos\phi \cos\phi' \cos(\lambda - \lambda'))$, (Data from [10]).

as a basis. The Love-numbers of [9], he utilized the Gutenberg-Bullen-Earth-Model, differ distinctly for large degrees n, from the above ones.

2.1.2 The Equations of Motion and the Equation of Continuity

The loading and self-attraction effect is described through the potential (2.8 and 2.6)

$$\Phi^* = V' + \Phi = \sum_{n=0}^{\infty} (1 + k'_n)\Phi_n = \sum_{n=0}^{\infty} g(1 + k'_n)\alpha_n \zeta_n \tag{2.9}$$

with $\alpha_n = \frac{3}{2n+1}\frac{\rho_0}{\rho_e}$, and the displacement of the ocean bottom δ (2.7).
The secondary force is given by the horizontal gradient ∇_H of this potential (2.9):

$$\mathbf{L}_{sek} = \nabla_H \Phi^* =: g\nabla_H \overline{\zeta} \tag{2.10}$$

There, $\overline{\zeta}$ is the equilibrium representation of the secondary potential. The sea level ζ relative to the moving sea bottom is described through the vertical displacement δ of the sea bottom and the geocentric sea level ζ_0:

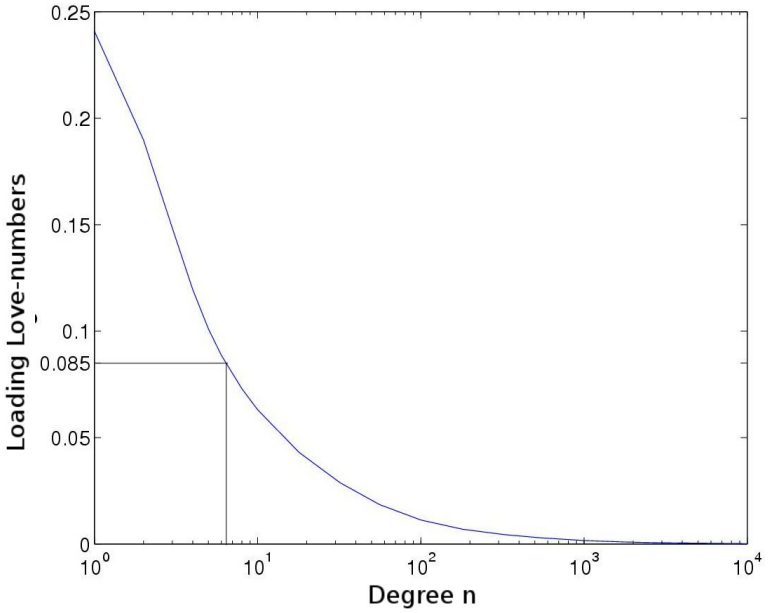

Fig. 2.4 The Love-number combination $(1+k'_n-h'_n)\alpha_n$. The abscissa shows the degree n of the spherical harmonic (Data from [9]). The value $(1+k'_n-h'_n)\alpha_n = 0.085$ is marked, which is often used for the parameterization of the LSA-effect [1].

$$\zeta_0 = \zeta + \delta \tag{2.11}$$

Putting (2.10) and (2.11) in (2.2)- (2.4), results in

$$\frac{\partial u}{\partial t} - 2\omega \sin\phi \cdot v + \frac{r'}{D}u - A_h \Delta u + \frac{g}{R\cos\phi}\frac{\partial \zeta}{\partial \lambda} = \frac{g}{R\cos\phi}\frac{\partial(\overline{\zeta}-\delta)}{\partial \lambda} \tag{2.12}$$

$$\frac{\partial v}{\partial t} + 2\omega \sin\phi \cdot u + \frac{r'}{D}v - A_h \Delta v + \frac{g}{R}\frac{\partial \zeta}{\partial \phi} = \frac{g}{R}\frac{\partial(\overline{\zeta}-\delta)}{\partial \phi} \tag{2.13}$$

To obtain a system of equations with the three state variables u, v and ζ, the spherical harmonics ζ_n must be expressed through ζ. Transformation of (2.5) results in

$$\begin{matrix} C_{n,s} \\ S_{n,s} \end{matrix} = \frac{1}{4\pi}\int\int \zeta(t,\lambda',\phi')\overline{P}_{n,s}(\sin\phi')\begin{matrix}\cos(s\lambda') \\ \sin(s\lambda')\end{matrix} d\lambda' d\phi' \cos\phi'$$

Finally, by substituting this into (2.12) and (2.13), the system of equations is rewritten as:

$$\frac{\partial u}{\partial t} - 2\omega \sin\phi \cdot v + \frac{r'}{D}u - A_h \Delta u + \frac{g}{R\cos\phi}\frac{\partial \zeta}{\partial \lambda} = \tag{2.14}$$

$$\frac{g}{R\cos\phi}\int\int \zeta(t,\lambda',\phi')\frac{\partial G(\lambda,\phi,\lambda',\phi')}{\partial\lambda}d\lambda' d\phi'\cos\phi'$$

$$\frac{\partial v}{\partial t}+2\omega\sin\phi\cdot u+\frac{r'}{D}v-A_h\Delta v+\frac{g}{R}\frac{\partial\zeta}{\partial\phi}= \tag{2.15}$$
$$\frac{g}{R}\int\int \zeta(t,\lambda',\phi')\frac{\partial G(\lambda,\phi,\lambda',\phi')}{\partial\phi}d\lambda' d\phi'\cos\phi'$$

$$\frac{\partial\zeta}{\partial t}+\frac{1}{R\cos(\phi)}\left(\frac{\partial(Du)}{\partial\lambda}+\frac{\partial(Dv\cos\phi)}{\partial\phi}\right)=0 \tag{2.16}$$

This is an integro-differential equation system. The function

$$\begin{array}{l}G(\lambda,\phi,\lambda',\phi'):=\\ \frac{1}{4\pi}\sum_{n=0}^{\infty}(1+k'_n-h'_n)\alpha_n\sum_{s=0}^{n}\overline{P}_{n,s}(\sin\phi)\overline{P}_{n,s}(\sin\phi')\cos(s(\lambda'-\lambda))\end{array} \tag{2.17}$$

contains the loading Love-numbers. This function is often called the Green's function of loading and self-attraction. An important characteristic of this Green's function is that its dependency on the four variables $(\lambda,\phi,\lambda',\phi')$ can be reduced to that on the angular distance a, given through

$$\cos a=\sin\phi\sin\phi'+\cos\phi\cos\phi'\cos(\lambda-\lambda').$$

This is possible since the Love-numbers, which are forming the basis of the Green's function are only depending on the degree of the spherical harmonics and not on their order. The proof is given through the so called addition-theorem of Legendre-polynomials ([45], page 427):

$$P_n(\cos a)=\sum_{s=0}^{n}\frac{(n-s)!2}{(n+s)!\delta_s}P_{n,s}(\sin\phi')P_{n,s}(\sin\phi)\cos(s(\lambda'-\lambda)) \tag{2.18}$$

Putting this expression in (2.17), the Green's function is rewritten in the form

$$G(a)=\frac{1}{4\pi}\sum_{n=0}^{\infty}(1+k'_n-h'_n)\alpha_n\overline{P}_n(\cos a). \tag{2.19}$$

The Green's function, determined by the loading Love-numbers of [10], is displayed in Figure (2.3).

2.1.3 Energy Balance

The equations of motion (2.2- 2.4) are transformed into the following energy equation (e.g. [56])[1]:

$$\underbrace{\tfrac{\partial}{\partial t}[\tfrac{1}{2}D(u^2+v^2)]}_{Kinetic\ Energy} - \underbrace{\frac{1}{2}\frac{\partial \zeta}{\partial t}(u^2+v^2)}_{Correction\ Term} + \underbrace{r'D(u^2+v^2)^{\frac{3}{2}}}_{Dissip.\ Bottom\ Friction} +$$
$$g\nabla\cdot\underbrace{(Du\zeta_0, Dv\zeta_0)}_{Energy\ Flux} - \underbrace{DA_h((\nabla u)^2+(\nabla v)^2) + DA_h(\nabla\cdot(u\nabla u + v\nabla v))}_{Dissipation\ Through\ Eddy\ Viscosity} +$$
$$\underbrace{\tfrac{\partial}{\partial t}(\tfrac{1}{2}g\zeta^2 + g\delta\zeta)}_{Potential\ Energy} = \tag{2.20}$$
$$\underbrace{\nabla\cdot(Du\Phi^*, Dv\Phi^*) + \Phi^*\frac{\partial\zeta}{\partial t}}_{Work\ Done\ Through\ LSA-effect} + \underbrace{g\zeta\frac{\partial\delta}{\partial t}}_{Work\ Done\ Through\ Bottom\ Deformation}$$

The terms on the right hand side of this equation, originating from the LSA-effect, are zero in the time-mean energy budget [57].
Now, a particular free oscillation with the frequency $i\sigma = \sigma_1 + i\sigma_2$ and its complex constituents u, v and ζ is considered. The real part of $i\sigma$, i.e. σ_1, determines the damping rate of the mode, with the energy decay time $\frac{1}{2\sigma_1}$ [64]. The eigenperiod $T_2 = \frac{2\pi}{\sigma_2}$ is given through the imaginary part σ_2.
In order to evaluating in (2.20) the potential and kinetic energy contents as well as the energy flux term, the real parts of the constituents u, v and ζ of the complex eigenfunction are used in the form

$$u = |u|e^{-\sigma_1 t}\cos(-\sigma_2 t + \Psi + \phi_u) \tag{2.21}$$
$$v = |v|e^{-\sigma_1 t}\cos(-\sigma_2 t + \Psi + \phi_v) \tag{2.22}$$
$$\zeta = |\zeta|e^{-\sigma_1 t}\cos(-\sigma_2 t + \Psi + \phi_\zeta). \tag{2.23}$$

There, Ψ is an arbitrary phase shift.
The ocean bottom deformation δ is obtained from the sea surface elevation making use of the corresponding Green's function and is likewise represented by the amplitudes and phases

$$\delta = |\delta|e^{-\sigma_1 t}\cos(-\sigma_2 t + \Psi + \phi_\delta).$$

[1] In order to obtain energies the equation has to be multiplied by ρ.

The Averaging Method

Considering the time-mean of a product of two periodic functions, e.g. u and ζ (2.21)- (2.23)

$$M_{\zeta u} := \frac{1}{T}\int_0^T dt(\zeta u).$$

Substituting the real functions and integrating over the time results in

$$M_{\zeta u} = \frac{1}{8\pi((\frac{\alpha}{\sigma})^2+1)}\left(1-e^{\frac{-4\pi\alpha}{\sigma}}\right)[\underbrace{\frac{2\alpha}{\sigma}\cos(\phi_u+\Psi)\cos(\phi_\zeta+\Psi)}_{depending\ on\ \Psi}+$$
$$\frac{\sigma}{\alpha}\cos(\phi_u-\phi_\zeta)-\underbrace{\sin(\phi_u+\phi_\zeta+2\Psi)}_{depending\ on\ \Psi}]|\zeta||u| \quad (2.24)$$

The eigenfrequency has here the notation $\alpha := \sigma_1$ and $\sigma := \sigma_2$. Obviously, the two marked terms in the equation for $M_{\zeta u}$, depend on the arbitrary phase shift Ψ. Of course, this is due to the damping factor. In case of no dissipation ($\alpha = 0$) these two terms would disappear:

$$M_{\zeta u}^{(without\ dissipation)} = \frac{1}{2}\cos(\phi_u-\phi_\zeta)|\zeta||u|$$

Averaging the resulting $M_{\zeta u}$ (2.24) over the interval $(0,2\pi)$ with respect to the phase Ψ makes it independent of Ψ:

$$\overline{M}_{\zeta u} = \frac{1}{2\pi}\int_0^{2\pi} d\Psi M_{\zeta u} = B\cdot\cos(\phi_u-\phi_\zeta)|\zeta||u| \quad (2.25)$$
$$B := \frac{1}{8\pi((\frac{\alpha}{\sigma})^2+1)}\left(1-e^{\frac{-4\pi\alpha}{\sigma}}\right)\left(\frac{\alpha}{\sigma}+\frac{\sigma}{\alpha}\right)$$

Potential and Kinetic Energy

Using (2.20) and (2.25) the time-mean of the potential and kinetic energy surrenders to

$$\overline{E}_p = B\cdot(\frac{1}{2}\rho g|\zeta|^2+\rho g|\delta||\zeta|\cos(\phi_\delta-\phi_\zeta)) \quad (2.26)$$
$$\overline{E}_k = B\cdot\frac{1}{2}\rho D(|u|^2+|v|^2), \quad (2.27)$$

The total energy is given through:

$$\overline{E}_t = \overline{E}_p+\overline{E}_k \quad (2.28)$$

Energy Flux

The time-mean of the two components J_u and J_v of the energy flux, is determined through (2.20) and (2.25):

$$\overline{J_u} = \rho g D(\overline{M}_{u\zeta} - \overline{M}_{u\delta}) = B \cdot \rho g D|u|(|\zeta|\cos(\phi_u - \phi_\zeta) - |\delta|\cos(\phi_u - \phi_\delta)) \quad (2.29)$$

$$\overline{J_v} = \rho g D(\overline{M}_{v\zeta} - \overline{M}_{v\delta}) = B \cdot \rho g D|v|(|\zeta|\cos(\phi_v - \phi_\zeta) - |\delta|\cos(\phi_v - \phi_\delta)) \quad (2.30)$$

2.1.4 Parameterization of the LSA - An Analytical Approach

Considering the shallow water equations (2.1) without friction and the LSA-effect, the so called Laplace-equations are given by:

$$\frac{\partial \mathbf{v}_H}{\partial t} + (\mathbf{f} \times \mathbf{v})_H = -g\nabla_H \zeta \quad (2.31)$$

$$\frac{\partial \zeta}{\partial t} + \nabla_H \cdot (D\mathbf{v}_H) = 0 \quad (2.32)$$

$$\mathbf{v}_H \cdot \mathbf{n}|_\Gamma = 0 \quad (2.33)$$

With the Operator $\mathscr{L}_0$

$$\mathscr{L}_0 = \begin{pmatrix} \mathbf{f}\times & g\nabla_H \\ \nabla_H \cdot D & 0 \end{pmatrix} \quad (2.34)$$

and with the vector $\mathbf{w} = \begin{pmatrix} \mathbf{v}_H \\ \zeta \end{pmatrix}$, the above equation system (2.31, 2.32) can be rewritten as:

$$\frac{\partial \mathbf{w}}{\partial t} = -\mathscr{L}_0 \mathbf{w} \quad (2.35)$$

The loading and self-attraction effect is now defined by a perturbation operator $\delta\mathscr{L}$. [23] showed with this perturbation formalism, that the variation of the frequency of a free oscillation through the LSA-effect is

$$\frac{\delta\sigma}{\sigma} = \frac{-\int dS \zeta_{LSA}\zeta^*}{\int dS|\zeta|^2} \cdot \frac{E_p}{E_t} = -\beta \cdot \frac{E_p}{E_t} \quad (2.36)$$

where E_p/E_t is the ratio of the potential energy to the total energy, σ the frequency and ζ^* the conjugate complex sea surface elevation of the free oscillation determined without the LSA-effect. ζ_{LSA} is defined by the LSA-term (compare 2.17):

$$\nabla\zeta_{LSA} = \nabla \int\int_S \zeta(t,\lambda',\phi')G(\lambda,\phi,\lambda',\phi')R^2\cos(\phi')d\lambda' d\phi'. \quad (2.37)$$

Since ζ and ζ_{LSA} are not exactly in phase the proportional constant β, defined through (2.36), has a complex value. However, the imagenary part is considerably smaller than the real part (the factor is less than 0.001). Therefore β is treated as a real value in the following. As will be shown later, the sign of β is positive and thus the consideration of the LSA-effect results in a decrease of the frequencies of the free oscillations. The relative magnitude of this frequency shift depends on the ratio of potential energy to the total energy and on the factor $\beta = \frac{\int dS \zeta_{LSA} \zeta^*}{\int dS |\zeta|^2}$.

Parameterization of LSA

This β-value is the same, which [1] introduced for parameterizing the LSA-effect in tidal models. There, the LSA-term of equation (2.37) is approximated by: [1] obtained for M_2 constituent $\beta = 0.085$. [33] gave different values for the most important semidiurnal and diurnal tidal constituents (see Table 2.1) and [41] recommends a higher value for the M_2 with $\beta = 0.12$.
The LSA-term is still interactive with ζ when represented in this simple form. Howewer, it is a massive simplification since it does mean for all Love-numbers that $(1 + k'_n - h'_n)\alpha_n = \beta$ (compare Fig. 2.4). Analysis of the local distribution of β shows that there are large differences of β between the open ocean and the coastal region [41, 48]. The values of β are small near land, and are getting large in open ocean areas. Further, [48] introduce a local $\beta_L(\lambda, \phi) = \frac{\zeta_{LSA}(\lambda,\phi)}{\zeta(\lambda,\phi)}$ and discuss its dependency on ocean depth and on latitude for different time scales generated through various forcings (tidal, atmospheric wind, atmospheric pressure) of their barotropic ocean model. For a detailed analysis of the β-values of the gravitational modes see Sections (3.1.1) and (3.1.2), and of the vorticity modes see Section (3.2).

$$\nabla \zeta_{LSA} \approx \beta \cdot \nabla \zeta \tag{2.38}$$

Table 2.1 β-values (2.36) for the most important semidiurnal and diurnal tidal constituents [33].

diurnal		semidiurnal	
K_1	0.121	M_2	0.082
O_1	0.115	S_2	0.083
P_1	0.119	N_2	0.079

2.2 Model

The physical model for the global free oscillations is described through the eigenvalue problem

$$-i\mathscr{L}\bar{\mathbf{w}} = \sigma\bar{\mathbf{w}} \tag{2.39}$$

$$\mathbf{v}_H \cdot \mathbf{n}|_r = 0 \tag{2.40}$$

here, the periodic function $\mathbf{w}(\lambda,\phi) = \begin{pmatrix} \mathbf{v}_H \\ \zeta \end{pmatrix} = \begin{pmatrix} \bar{\mathbf{v}}_H \\ \bar{\zeta} \end{pmatrix} \cdot \exp(-i\sigma t)$, with the complex valued frequency $i\sigma = \sigma_1 + i\sigma_2$ is introduced. The operator $\mathscr{L}$, derived from the system of equations (2.14- 2.16), is

$$\mathscr{L} = \begin{pmatrix} \mathbf{f}\times + \frac{r'}{D} - A_h\Delta_H & g\nabla_H - g\nabla_H\mathscr{I} \\ \nabla_H \cdot D & 0 \end{pmatrix}, \tag{2.41}$$

where $\mathscr{I}$ is defined through $\mathscr{I}\zeta = \int G(\lambda,\phi,\lambda',\phi')\zeta(\lambda',\phi')d\lambda' d\phi' \cos\phi'$.
Properly replacing the derivatives by finite differences and the integral by a finite expression [61] makes (2.39) turn into a system of algebraic equations

$$(A - \lambda I)\mathbf{x} = 0 \tag{2.42}$$

where $\lambda = i\sigma = \sigma_1 + i\sigma_2$ represents the eigenvalue of the Matrix A with the corresponding eigenvector $\bar{\mathbf{x}} = \mathbf{x}e^{-i\sigma t}$ depending on space as well as on time, i.e. $\bar{\mathbf{x}} = \bar{\mathbf{x}}(t,\lambda,\phi)$.
The system of equations (2.42) has, in the present case of a spatial resolution of one degree, approximately 120,000 unknowns. Since LSA is taken fully into account the entries of the matrix A are generally nonzero. However, since the Green's function depends only on the angular distance a, symmetries in the arrangement of the entries can be utilized to reduce the working memory of the model to less than 1GB (compare equation 2.19). Taking advantage of this memory reduction, three single free oscillations were computed with a special modification of the Wielandt Method Wielandt Method [64] and four with the standard Wielandt method [29]. In the first case the model was time optimized with respect to the method itself, whereas in the latter one it was distributed with OpenMP on 8 cpus and optimized for the HLRE[2].
Both approaches make use of the Wielandt Method (or inverse iteration), as described in [13] and as originally having been developed by [55], see also [17]. Starting from a first guess eigenvalue σ_0, the method yields the free oscillation with the eigenvalue λ closest to σ_0. The advantage of this method is that single free oscillations are determined with comparable low computational costs due to the possibility of the above mentioned memory reduction. The main disadvantage is the time consuming procedure when allowing for the full LSA-effect and that not all free oscillations are captured by this method.

[2] HLRE - High Perfomance Computing Centre for Earth System Research, Hamburg.

2.2.1 The Implicitly Restarted Arnoldi Method

In the present study the Implicitly Restarted Arnoldi Method is used for solving the eigenvalue problem (2.39). It is provided by the software package ARPACK [20]. The original Arnoldi Method [2] is an orthogonal projection method, belonging to the class of Krylov subspace methods. In case of a symmetric Matrix A, it reduces to the Lanczos Method [19]. Below, only a short summary of the Arnoldi method is given. A more comprehensive treatment of the subjects of Krylov subspaces, Arnoldi factorization, and Arnoldi method can be found in [43].

The k-th Krylov subspace associated with the matrix A and the vector $\mathbf{v}$ is defined through

$$\mathscr{K}_k(A,\mathbf{v}) = span\{\mathbf{v}, A\mathbf{v}, A^2\mathbf{v}, ..., A^{k-1}\mathbf{v}\}. \tag{2.43}$$

Obviously, it is defined through the sequence of vectors produced by the power method (e.g. [13]). This method utilizes the fact that with k increasing the vector $A^k\mathbf{v}$ converges to the eigenvector with the largest eigenvalue. Like all Krylov subspace methods, the Arnoldi method takes advantage of the structure of the vectors produced by the power method, and information is extracted to enhance convergence to additional eigenvectors. For this purpose, the Arnoldi method determines an orthonormal basis $span\{\mathbf{u}_1, \mathbf{u}_2, ...\mathbf{u}_k\}$ for $\mathscr{K}_k(A,\mathbf{v})$. This basis is defined through the relation

$$AU_k = U_k H_k + \mathbf{f}_k \mathbf{e}_k^T \tag{2.44}$$

where $A \in \mathbf{C}^{n\times n}$, the matrix $U_k = (\mathbf{u}_1, \mathbf{u}_2, ...\mathbf{u}_k) \in \mathbf{C}^{n\times k}$ (has orthogonal columns), $U_k^H \mathbf{f}_k = 0$, $\mathbf{e}_k \in \mathbf{C}^k$ and $H_k \in \mathbf{C}^{k\times k}$ is upper Hessenberg with non-negative subdiagonal elements. This is called a k-step Arnoldi factorization and its algorithm is shown in Fig. 2.5. Alternatively, the factorization (2.44) can be written as

$$AU_k = (U_k, \mathbf{u}_{k+1}) \begin{pmatrix} H_k \\ \beta_k \mathbf{e}_k^T \end{pmatrix}, \tag{2.45}$$

where $\beta_k = \|\mathbf{f}_k\|$ and $\mathbf{u}_{k+1} = \frac{1}{\beta_k}\mathbf{f}_k$. If $H_k\mathbf{s} = \mathbf{s}\theta$ then the vector $\mathbf{x} = U_k\mathbf{s}$ satisfies

$$\|A\mathbf{x} - \mathbf{x}\theta\| = \|(AU_k - U_k H_k)\mathbf{s}\| = |\beta_k \mathbf{e}_k^T \mathbf{s}|. \tag{2.46}$$

The so called Ritz-pair $(\mathbf{x}, \theta)$ is an approximate eigenpair of A, with the Ritz-estimate as the residual $r(\mathbf{x}) = |\beta_k \mathbf{e}_k^T \mathbf{s}|$ (assuming $\|\mathbf{x}\| = 1$).

Unfortunately, the Arnoldi Method has large storage and computational requirements. Large memory is used to store all the basis vectors u_k, if the number of iteration steps k is getting large before the eigenvalues and eigenvectors of interest are well approximated through the Ritz-pairs. Additionally, the computational cost of solving the Hessenberg eigenvalue subproblem rises with $\mathscr{O}(k^3)$. To overcome these difficulties, methods have been developed to implicitly restart the method [47]. This efficient way to reduce the storage and computational requirements makes the Arnoldi Method suitable for large scale problems. Further, implicit restarting pro-

Input $(A, \mathbf{v})$

Put $\mathbf{u}_1 \mathbf{v}/\|\mathbf{v}\|$; $\quad \mathbf{w} = A\mathbf{u}_1$; $\quad \alpha_1 = \mathbf{u}_1^H \mathbf{w}$;

Put $\mathbf{f}_1 \leftarrow \mathbf{w} - \mathbf{u}_1 \alpha_1$; $\quad U_1 \leftarrow (\mathbf{u}_1)$; $\quad H_1 \leftarrow (\alpha_1)$

For $j = 1, 2, 3, \ldots k-1$

(1) $\beta_j = \|\mathbf{f}_j\|$; $\quad \mathbf{u}_{j+1} \leftarrow \mathbf{f}_j/\beta_j$;

(2) $U_{j+1} \leftarrow (U_j, \mathbf{u}_{j+1})$; $\quad \widehat{H}_j \leftarrow \begin{pmatrix} H_j \\ \beta_j \mathbf{e}_j^T \end{pmatrix}$;

(3) $\mathbf{w} \leftarrow A\mathbf{u}_{j+1}$;

(4) $\mathbf{h} \leftarrow U_{j+1}^H \mathbf{w}; \mathbf{f}_{j+1} \leftarrow \mathbf{w} - U_{j+1}\mathbf{h}$;

(5) $H_{j+1} \leftarrow (\widehat{H}_j, \mathbf{h})$;

End For

Fig. 2.5 Algorithm: The k-step Arnoldi Factorization.

vides a means to determine a subset of the eigensystem. Hence, the ARPACK interface allows the user to specify the number l of eigenvalues sought.
When the Matrix A is considered in the Arnoldi method its l largest eigenvalues are determined. But in the case of the present study the interest lies in specific eigenvalues, e.g. those in the diurnal and semidiurnal spectrum. Therefore the shifted and inverted problem $(A - \sigma_0 I)^{-1}$is considered. Thus the convergence of eigenvalues near the selected point σ_0 is enhanced. This approach is closely related to the inverse iteration techniques (e.g. [13]). Considering this spectral transformation in detail yields

$$A\mathbf{x} = \mathbf{x}\lambda \Longleftrightarrow (A - \sigma_0 I)\mathbf{x} = \mathbf{x}(\lambda - \sigma_0). \tag{2.47}$$

and

$$(A - \sigma_0 I)^{-1}\mathbf{x} = \mathbf{x}\nu, \; \textit{where } \nu = \frac{1}{\lambda - \sigma_0}. \tag{2.48}$$

Hence, the eigenvalues λ that are close to σ_0 will be transformed into eigenvalues $\nu = \frac{1}{\lambda - \sigma_0}$, which are at the extremes of the transformed spectrum. The corresponding eigenvectors remain unchanged.
In case of the shifted and inverted approach of the Arnoldi Method, linear systems of the form $(A - \sigma_0 I)\mathbf{x} = b$ have to be solved. The algorithms of ARPACK are provided with a so called *reverse communication interface*. This interface allows the user to transfer the solution $\mathbf{x}$ into the algorithm, and in this way the solver can be chosen independently from ARPACK. In the present study the LU-solver provided by ScaLAPACK [4] is used (see next section). The LU-solver puts itself forward since the time consuming LU-factorization of $(A - \sigma_0 I)$ need to be performed only once.

2.2.2 The Parallelization with MPI

To enable the use of routines of mathematical libraries for computing linear systems, it is necessary to store the complex matrix $(A - \sigma_0 I)$ in a general form. Thus the advantages of the symmetries of the matrix are getting lost. Since more than 500 GB of memory are required, it is necessary to parallelize the ocean model and distribute the matrix on different nodes. The parallization is done with MPI[3], perfect for large problems needing access to large amounts of memory on distributed memory architectures [46].
The linear systems are solved with a parallelized version of a LU-solver of the ScaLAPACK software package [4]. Since the Matrix $(A - \sigma_0 I)$ is kept preserved during the whole iteration process of the Arnoldi algorithm, the LU-factorization, the most time consuming part, is only performed once. The choice of MPI and the ScaLAPACK LU-solver gives the user a high degree of freedom, in adapting the ocean model to the features of the computer architecture. The number of CPUs and nodes can freely be chosen, and is only restricted through the memory used to store the matrix.

2.2.3 The Performance of the Model

The model-runs have been performed on two distinct supercomputers, the HLRE[4] and the HLRS[5], equipped with NEC SX-6 nodes and NEC SX-8 nodes, respectively.
The number of free oscillations sought is set to $l = 150$ for each model-run. So

Table 2.2 Data of the performance of the fastest model-run on 12 NEC SX-6 nodes of the HLRE: First two rows shows values from one single cpu; last row are mean global values of all 96 cpus.

	Frequency	Time in $[s]$	Performance in $[MFlops]$
LU-factorization (of cpu no. 1)	1	6872.6	6766.8
LU-solver (of cpu no. 1)	500	444.7	1373.1
Mean global values of 96 cpus		8181.2	$608.7 \cdot 10^3$

[3] Message-Passing Interface.

[4] HLRE - High Perfomance Computing Centre for Earth System Research, Hamburg.

[5] HLRS - High Performance Computing Centre, Stuttgart.

75 free oscillations and the corresponding complex conjugated ones are computed. At the HLRE it is possible to run the program on 12 and 16 nodes. Each SX-6 is equipped with 8 cpus. The overall performance is up to 609 and 632 GFlops, respectively, being one of the fastest single-application running on the HLRE. The computation time is between 2 and 3 hours, mostly depending on the actual state of the supercomputer and on the condition of the matrix, which changes through changing σ_0 value. Although the LU-factorization is highly optimized (Table 2.2), it alone needs more than two third of the total time used by the model (in some cases up to 80%), the LU-solver uses 5-8%. The total memory of the model amounts to 630GBytes.

Furthermore, model-runs have been performed on the HLRS supercomputer. It is

Table 2.3 Data of the performance of model-runs on 4, 8, 16, 32 and 64 NEC SX-8 nodes of the HLRS.

Number of nodes	4	8	16	32	64
Number of cpus	32	64	128	256	512
Real Time in $[s]$	11421	6850	4463	3251	2766
Performance in $[GFlops]$	416	737	1269	2108	3394

one of the TOP 100 Supercomputers of the world[6], and ranked 48th in July 2006[7]. The model was distributed on up to 512 cpus (64 nodes). On this computer architecture the good performance of the model is kept preserved (Table 2.3), using only 45 minutes to determine 150 normal modes, with a mean performance of 3.4TFlops.

[6] http://www.top500.org/.

[7] The date when these model-runs have been performed.

http://www.springer.com/978-3-540-85575-0

A Large Spectrum of Free Oscillations of the World Ocean Including the Full Ocean Loading and Self-attraction Effects

Müller, M.

2009, XII, 120 p., Softcover
ISBN: 978-3-540-85575-0